

Reaction Mechanism and Kinetics of the Atmospheric Reactions of 2, 3-Dimethylphenol with OH Radical*

L. Sandhiya, P. Kolandaivel and K. Senthilkumar

Department of Physics

Bharathiar University, Coimbatore, India-641 046

Email: ksenthil@buc.edu.in

(Received June 14, 2011)

Abstract: Aromatic compounds such as benzene, toluene and xylene are important constituents of gasoline fuels, solvents and are ambient air pollutants in urban areas. The atmospheric degradation of xylene leads to the formation of dimethylphenols, which are highly reactive in the atmosphere. The dominant degradation process for dimethylphenols is their reaction with OH radical, which proceeds by H-atom abstraction from the alkyl substituted groups. The resulting alkyl radical further undergo oxidation reaction with O₂, leading to the formation of an alkyl peroxy radical. This alkyl peroxy radical further reacts with atmospheric species to generate new products. In the present work, the possible ring cleaving reaction mechanism for OH initiated reaction of 2,3-dimethylphenol is studied, the different reaction pathways are modeled, and the major product channels are identified by theoretical methods. The potential energy surface for the reaction system is characterized by using DFT-B3LYP/6-31G(d,p) level of theory. The connectivity of the transition states with their corresponding reactants and products is confirmed by intrinsic reaction coordinate calculations. The rate constants of the reaction channels are calculated using canonical variational transition state theory (CVT) with small curvature tunneling (SCT) corrections over the temperature range of 278-350 K. The formation of 3-hydroxy-2-methyl-2H-pyran-2-carbaldehyde is found to be favorable with a small energy barrier of 7.74 kcal/mol and with a rate constant of $2.22 \times 10^{-11} \text{ cm}^3 \text{ molecule}^{-1} \text{ s}^{-1}$ at 298 K. Thus, the peroxy radical chemistry achieves the conversion of dimethylphenol to unsaturated dicarbonyls and aldehydes, thereby aiding oxidation and combustion processes that either releases large amount of energy or form reactive free radicals.

Keywords: Dimethylphenols, oxidative degradation, barrier height, rate constant.

1. Introduction

Aromatic compounds such as benzene, toluene and xylene are vital air pollutants in urban areas. Exceptional use of automobile fuel results in

*Paper presented in CONIAPS XIII at UPES, Dehradun during June 14-16, 2011.

substantial emissions of aromatic compounds into atmosphere¹⁻³. The atmospheric degradation of these aromatics is initiated through oxidation reaction by OH radical⁴⁻⁵. Understanding the oxidation chemistry of aromatic compounds is important, because this reaction is responsible for photochemically produced tropospheric ozone⁶. The oxidation of aromatic compounds leads to the formation of secondary aerosols, which have particular concern on human health and climate⁷. The reaction of aromatic compounds with OH radical produces cresols, phenols and dimethylphenols⁸. Hence, in order to understand the environmental implications of aromatic compounds present in the atmosphere, a detailed study of the degradation mechanism of these products is very essential. Also, an accurate modeling of the reaction mechanism will provide information about the degradation products and their lifetimes.

Among the aromatic compounds, dimethylphenols are formed due to the oxidation of xylene by OH radical in the atmosphere. They are also obtained from coal tar or petroleum as by-products in the fractional distillation and in coal gasification³. Dimethylphenols are related to various health hazards such as cardiovascular, respiratory and skin toxicants. Hence, it is very important to know whether dimethylphenol remain as such in the atmosphere or it will degrade into new products which can be harmless, less harm or even hazardous to life on earth. The atmospheric degradation of aromatic compounds proceeds via complex pathways which generate a large number of products. Few smog chamber experiments have focused on identifying the products formed during the atmospheric degradation of dimethylphenol⁹⁻¹⁰. However, through experimental studies, this is very challenging as the simultaneous identification and quantification of the large number of chemically similar products is a difficult task. To overcome this difficulty, quantum chemical methods provide the best tools to identify and characterize the complex degradation pathways. Despite its recognized importance and a great deal of scientific study, the atmospheric degradation of dimethylphenol remains unclear. In view of the above mentioned exposures and the practical importance of the degradation of dimethylphenol by OH radicals, the principal aim of this work is to characterize the full potential energy surface of the reaction system by carefully mapping out the various degradation processes using computational methods.

In the present work, the reaction between 2,3-dimethylphenol and OH radical is studied, which is initiated through abstraction of H-atom present in the phenol group or methyl group of 2,3-dimethylphenol by OH radical. The H-atom abstraction from phenolic group further undergoes secondary reaction with O₂ leading to the formation of 2,3-dimethylphenol-benzoquinone¹¹. As shown in Scheme 1, the H-atom abstraction from methyl

group results in the formation of an alkyl radical. The initially formed alkyl radical is found to react more rapidly with O_2 and a peroxy radical is formed which is the major transformation in the troposphere¹²⁻¹⁴. At lower temperature, this peroxy radical is stabilized by bath gas collisions and is able to participate in further bimolecular reactions. This peroxy radical is the key intermediate in the reaction mechanism and has excess energy to further undergo reaction with HO_2 in the atmosphere leading to the formation of new compounds. As shown in Scheme 1, the reaction between peroxy radical and HO_2 leads to the formation of formic acid, 3-methylphenol and O_2 . The formic acid so formed contributes significantly to the acidity of atmospheric precipitation and is further degraded by atmospheric heterogeneous transformations¹⁵. The 3-methylphenol further undergoes oxidation reaction with O_2 leading to the formation of organic compounds such as dicarbonyls, aldehydes and alcohols. These products can further decompose to glyoxal and butanedial which are the principal oxidation products of aromatic compounds¹⁶⁻¹⁷.

The secondary reactions of peroxy radical with HO_2 slow down the free radical driven photochemical oxidation reactions and reduce the formation of ozone. Also, these reactions represent an important chemical sink for HO_x radicals in the troposphere. Hence, the reactions of peroxy radical with HO_2 are of comparable importance in the atmospheric fate of dimethylphenols. Previous studies on the reactions of dimethylphenol with OH radical have focused only on the initial H-atom abstraction step and its kinetics⁹⁻¹⁰. To date, no detailed study regarding the reaction mechanism, degradation products, and kinetics of the subsequent reactions of dimethylphenol with OH radical is available in the literature. Hence, this work mainly focused on the study of possible pathways of the reaction between 2,3-dimethylphenol and OH radical which leads to the formation of several products of environmental concern. Theoretical calculations using density functional theory have been performed in this work aiming to assess the feasibility of the reaction channels and to provide thermochemical data for the reaction system. The transition states corresponding to possible intermediates and products are located to identify the reaction pathways. Also, in order to predict the lifetime of dimethylphenol emitted into the atmosphere, the rate constants over the temperature range of the troposphere, for the reactions involving major product channels are determined using Variational Transition State Theory.

2. Computational Methodology

The geometry of the reactant, intermediates, transition states and products on the potential energy surface of the reaction system of

dimethylphenol with OH were optimized by the hybrid density functional B3LYP method¹⁸⁻¹⁹ with the 6-31G(d,p) basis set. Previous studies on atmospheric reactions show that the structures and energies obtained with B3LYP method is comparable with the results of MP2, CCSD(T) and QCISD methods²⁰⁻²¹. In the present work, B3LYP/6-31G(d,p) level of theory is used to obtain the structure and energy of the reacting species. The same method was used to obtain vibrational frequencies and zero-point energy (ZPE) corrections and to characterize the stationary points as minima or first order saddle points. Global minima were confirmed with all positive frequencies, while each transition state had one imaginary frequency confirming their maxima in one reaction coordinate. Intrinsic reaction coordinate (IRC) calculations²² were carried out in each case to confirm that the transition state structures connect the designated reactant and product. The paths were computed following the second order algorithm of Gonzalez and Schlegel²³. The energy derivatives including gradients and Hessians at geometries along the minimum energy path (MEP) were also obtained. The barrier height and enthalpy of reaction were calculated by including thermodynamic corrections to the energy at 298.15 K. All the electronic structure calculations were performed using Gaussian 09 program package²⁴.

The potential energy surface, gradients and Hessians obtained from electronic structure calculations were directly used to calculate the rate constants. The theoretical rate constants for the reactions were calculated using canonical variational transition state theory (CVT)²⁵⁻²⁶. The tunneling correction defined as the Boltzmann average of the ratio of the quantum and classical probabilities was calculated using small curvature tunneling (SCT) method²⁷⁻²⁸. Through canonical variational transition state theory, the rate constant at temperature T is given by

$$(1.1) \quad k^{CVT}(T) = \min_s k^{GT}(T, s),$$

where

$$(1.2) \quad k^{GT}(T, s) = \frac{\sigma k_B T}{h} \frac{Q^{GT}(T, s)}{\phi^R(T)} e^{-V_{MEP}(s)/k_B T},$$

where $k^{GT}(T, s)$ is the generalized transition state theory rate constant at the dividing surface s , σ is the symmetry factor accounting for the possibility of more than one symmetry related reaction path, k_B is Boltzmann's constant, h is Planck's constant, $\phi^R(T)$ is the reactant partition function per unit volume, and $Q^{GT}(T, s)$ is the partition function of a generalized transition state at s .

The generalized normal-mode analysis is performed in Cartesian coordinates. The lowest vibrational mode of the transition state is treated as a hindered rotation, and all other vibrations are treated harmonically. The hindered rotor approximation²⁹ is used to calculate the partition function of the lowest vibrational mode. The rate constant calculations were performed by combining GAUSSRATE 2009A and POLYRATE 2010A programs³⁰⁻³¹.

3. Results and Discussions

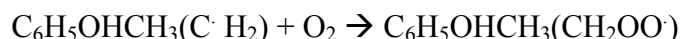
A. Reaction Mechanism and reaction paths:

The relative energy profile corresponding to different pathways of the reaction system is shown in Figure 1. The structure of stationary points on the ground-state potential energy surface of the reaction system optimized at the B3LYP/6-31G(d,p) level of theory is shown in Figure 2. The enthalpy (ΔE), Gibb's free energy (ΔG) and barrier height of the reactive species with ZPE corrected are summarized in Table 1. The intermediates, transition states and products are labeled as I, TS and P, respectively, followed by a number. The atoms are numbered as shown in Figure 2.

2, 3-dimethylphenol has two active sites for the reaction with hydroxyl group. The reaction between 2, 3-dimethylphenol and OH radical is initiated by H-atom abstraction from phenol group or from methyl group of 2,3-dimethylphenol by OH radical. Earlier studies on reaction of aromatic compounds with OH radical show that the reactions are initiated by electrophilic addition of OH radical to the aromatic ring [10, 32]. But in the case of 2, 3-dimethylphenol, the hydroxyl group is considerably more reactive than CH₃ groups. However, the presence of methyl groups provides steric hindrance to electrophilic addition of OH directly to the aromatic carbon atoms. Thus, the reaction between 2, 3-dimethylphenol and OH radical is found to occur more favorably by H-atom abstraction from methyl group.

The initial H-atom abstraction reaction results in the formation of an alkyl radical I1 with the elimination of a water molecule. This abstraction reaction is characterized by a transition state TS1 with a very small barrier of 3.94 kcal/mol. In the transition state structure TS1, the angle between the H-atom of CH₃ group and the reacting OH radical is found to be 130° which was 92° in the reactants. Also, the distance between the H-atom of CH₃ group and the O-atom of OH decreased by 0.5 Å from that of the reactants. This initial reaction is exothermic by -27.35 kcal/mol, as observed for other H-atom abstraction reactions in earlier studies³³⁻³⁵. This reaction is endoergic with a small free energy of 0.9 kcal/mol. The alkyl radical formed in the initial step is found to undergo a secondary reaction with O₂ and this results

in the formation of peroxy radical intermediate I2. This intermediate is formed through a transition state TS2 with a small with a negative activation barrier of 16.3 kcal/mol. The distance between the carbon atom in methyl radical site and O-atom of O₂ in the transition state structure TS2 decreased by 1.6 Å from that of the reactants. Also, in the intermediate I2, the distance between the carbon atom in methyl radical and O-atom is found to be 0.2 Å lesser than that of the transition state TS2. This intermediate is formed exothermically with an enthalpy of -21 kcal/mol. This exothermicity is similar to the benzylperoxy radical formation in a mild exothermic reaction with a value of -20 kcal/mol³⁶. The reaction is endoergic with ΔG=6.9 kcal/mol. The associated reactions are



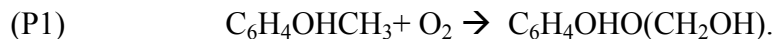
As shown in Scheme 1, the peroxy radical thus formed further reacts with HO₂ leading to the formation of 3-methylphenol, formic acid and O₂. The O-atom of peroxy group abstracts H-atom from HO₂ and the distance between the C-atom in the second position and the C-atom attached to the peroxy group is increased by 2 Å and is therefore cleaved. Thus HCOOH group is removed and the remaining H-atom in the radical makes a new bond with the C-atom in the second position of C₆H₃OH(CH₃) [see Figure 2]. Thus, the intermediate 3-methylphenol (I3) is formed. These products are formed via a transition state TS3 with a barrier of 30.5 kcal/mol. In the transition state structure TS3, the bond between the H and O atoms of HO₂ is elongated by 1 Å and a weak hydrogen bonding is observed between O-atom of HO₂ and H-atom of phenol group of peroxy radical. This reaction occurs in a highly exothermic process with an enthalpy of -86.02 kcal/mol, and with a free energy of -4.31 kcal/mol. This high exothermicity implies that the products formed in this reaction are highly activated with sufficient energy to proceed with secondary reactions to form new decomposition products. The associated reaction is,



The 3-methylphenol formed in this reaction serves as a key intermediate for the formation of ring cleavage products. The 3-methylphenol can predominantly undergo subsequent reactions with O₂ to form to new degradation products. The possible reactions are characterized by eight degradation pathways and are discussed below.

Pathway 1:

The reaction between the intermediate I3 and O₂ leads to the formation of 6-hydroxymethyl-oxa-bicyclo [4,1,0] hepta-2,4-diene-2-ol (P1) through a transition state TS4 with a negative activation barrier of 40.64 kcal/mol. Here the energy barrier is negative because the transition state TS4 is stabilized by the radical-induced dipole interactions between the reactants. As shown in Figure 2, in the transition state structure TS4, one of the O-atoms of O₂ forms a triangular structure with the carbon atom C1-atom and with its neighboring C2-atom from which the formic acid group was eliminated. Also, the other O-atom forms triangular structure with the fourth and sixth position C-atoms. This unstable structure further rearranges to form an alcoholic compound as shown in Figure 2. The C-O bond of COC-group attached to phenolic group in TS4 elongates by 1 Å and the O-atom makes a new bond with the aromatic C-atom to which the methyl group is attached, thereby forming a triangular structure. The O-atom bonded with this aromatic C-atom migrates and one of the H-atoms of CH₃ group shifts its position to bind with this O-atom and thus an alcoholic product is formed. This reaction occurs in a highly exothermic process with the products lying 51.8 kcal/mol below the reactants. As reported in Table 1, this product channel is endoergic by 3.5 kcal/mol. The reaction involved is

**Pathway 2:**

The second pathway involves the formation of 2-hydroxy-cyclopenta-2,4-dienecarboxylic acid methyl ester (P2). This reaction is characterized by a transition state TS5 with an energy barrier of 60.8 kcal/mol. In the transition state structure TS5, the C-C bond in the second and sixth positions of the aromatic ring loses its aromaticity and the O₂ molecule gets bonded with the C-atom in the fourth position and thus a peroxy group is formed. As shown in Figure 2, this transition state TS5 further rearranges itself and the bond between the fourth and sixth position C-atoms is cleaved and a new bond is formed between the C-atoms in the second and sixth positions. Also, one of the O-atoms of peroxy group bifurcates the C-C bond between the fourth position C-atom and that of the methyl group in order to form C-O-C group and the other O-atom makes a double bond with that of the C-atom in the fourth position. Thus, a neutral product is formed. This product channel is formed exothermically with a reaction enthalpy of -76.83 kcal/mol and the reaction is endoergic with a free energy of 3.18 kcal/mol. This reaction is not

so feasible due to the pronounced barrier height of TS5. The corresponding reaction is



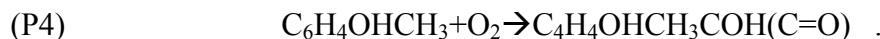
Pathway 3:

The next reaction is the aromatic ring opening leading to a neutral product 2-hydroxy-cyclohept-4-ene-1,3-dione (P3). In this reaction, the bond between the sixth position C-atom and that of the methyl group is broken, and the C-atom of methyl group makes new bond with that of the aromatic C-atom and therefore a circular structure is formed. As shown in Figure 2, the H-atoms attached to the C-atoms shift their positions and the reacting O₂ molecule is also cleaved. The O-atoms then get bonded with the C-atoms in which the H-atoms were lost and possess double bond character. This ring opening and rearrangement reaction occurs through a transition state TS6 whose barrier is found to be -40.57 kcal/mol. The transition state structure TS6 is an aromatic structure in which the reacting O₂ molecule thereby splits into two O-atoms and binds inductively with the aromatic C-atoms. As given in Table 1, this reaction is also a highly exothermic reaction with reaction enthalpy of -85.12 kcal/mol and a free energy of 3.82 kcal/mol. The reaction involved is



Pathway 4:

This pathway includes continuous association and disassociation processes, which leads to a complete ring breaking reaction and an open chain product 7-hydroxy-hepta-4,6-diene-2,3-dione (P4) is formed. This reaction occurs via a transition state TS7 with a potential barrier of 29.4 kcal/mol. In the transition state TS7, the reacting O₂ molecule is cleaved and one of the O-atoms gets bonded between the first and second position C-atoms of I3, while the other O-atom forms a triangular structure with the fourth and sixth position C-atoms. Also, the O-atom bonded between the first and second positions forms an intermolecular hydrogen bonding with the H-atom bonded to the C-atom in the second position. Further, as shown in Figure 2, this transition state structure disassociates into a neutral product. This open chain product can again degrade to form important products like methyl glyoxal and butanol. This reaction channel is highly exothermic by 79.21 kcal/mol and the reaction occurs in a mild exoergic process with a small free energy of -0.18 kcal/mol. The corresponding reaction is



Pathway 5:

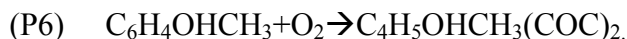
This reaction occurs through breaking of the C-C bond between C4 and C2 of the methyl group attached to it, and forming the C-C bond between the second position C-atom and C-atom of the methyl group of I3. The reacting O₂ molecule again splits and one of the O-atoms get bonded between the fourth and sixth position C-atoms and the other O-atom possess double bond character with that of the second position C-atom. Thus an aldehyde product 3-hydroxy-2-methyl-2H-pyran-2-carbaldehyde (P5) is formed [see Figure 2]. Three transition state structures (TS8, TS8', TS8'') were identified for this reaction channel. As shown in Figure 2, the geometries of these transition states essentially differ from one another based on the orientation of the O-O bond of O₂ with respect to C-C bonds of I3. In the transition state structure TS8, the O₂ molecule is aligned in plane with respect to the C-atoms in the first and sixth positions of I3 with an energy barrier of 8.39 kcal/mol above the reactants. In the transition state structure TS8', the bond between the fourth and sixth position C-atoms of I3 is cleaved and one of the O-atoms binds between the two C-atoms. The other O-atom binds with the C-atom in the first position of I3. This transition state TS8' involves a small barrier of 7.74 kcal/mol. In the transition state structure TS8'', one of the O-atoms binds between the first and second position C-atoms and the other O-atom binds between the fourth and sixth position C-atoms of I3, with a negative activation barrier of 22.41 kcal/mol. Of the three transition state structures, this reaction is found to occur likely through TS8' due to its small barrier of 7.74 kcal/mol, and therefore this reaction is kinetically accessible. This product channel is also exothermic by 71.94 kcal/mol and the is endoergic with ΔG=2.88 kcal/mol. The corresponding reaction is



Pathway 6:

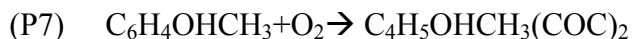
The next significant pathway leads to the formation of 7-methyl-2,8-dioxa-bicyclo[5,1,0]octa-3,5-diene-3-ol (P6). Here, the reacting O₂ molecule is cleaved and one of the O-atoms binds between the C-atoms in the first and second positions and the other O-atom forms a triangular structure between the second and fourth position C-atoms of I3. This product channel is formed through a transition state TS9 with a barrier of 8.39 kcal/mol above the reactants. The structures of TS9 and TS8 are similar except a small decrease

in distance between the sixth position C-atom of I3 and O-atom of O₂ in TS9 by about 0.3 Å from that of TS8. This reaction is the second most favorable due to a small barrier of 8.39 kcal/mol. This product is formed in an exothermic reaction with $\Delta H = -56.08$ kcal/mol and the reaction is endoergic by 3.09 kcal/mol. The reaction involved is



Pathway 7:

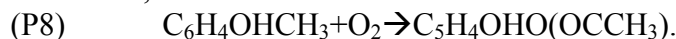
The reaction between I3 and O₂ can also lead to an adduct formation in which the O₂ molecule is cleaved and the O-atoms get attached between the aromatic C-atoms as shown in Figure 2. Thus, the product 2-methyl-[1,4] dioxocin-5-ol (P7) is formed. These compounds are relatively stable global pollutants and are very hazardous. This product formation is associated with a transition state TS10 with a barrier of 22.41 kcal/mol below the reactants. In the transition state structure TS10, the C-O bond distance is greater by 0.5 Å than that of the product. This reaction is exothermic by 50.61 kcal/mol and is endoergic with a free energy of 2.22 kcal/mol. The barrier for this reaction is considerably small and hence this reaction is energetically favorable. The process involved is



Pathway 8:

This pathway involved a complicated structural rearrangement of I3 on reaction with O₂. One of the O-atoms of O₂ acquires double bond character with the sixth position C-atom and the other O-atom bifurcates the bond between first and second position C-atoms and attaches exactly halfway between them. The distance between the first and sixth position C-atoms is contracted and a new bond is formed between them, resulting in the formation of 1-(1-hydroxy-2-oxa-bicyclo [2,2,0] hex-5-en-3-yl)-ethanone (P8). This complex product formation occurs through a small barrier of 12.06 kcal/mol at the transition state TS11. Such a small barrier favors this product formation. As shown in Figure 2, the transition from the reactants to the product involve the formation of a five-membered ring in which the CH₃ group attached in the fourth position of I3 shifts its position and binds with the second position C-atom. Also, the reacting O₂ molecule becomes cleaved and one of the O-atoms makes bond with C-atom in the first position and the other O-atom binds with C4-atom. This reaction is the least exothermic channel among all the studied reactions with an exothermicity of 40.43

kcal/mol and this reaction is endoergic by 1.66 kcal/mol. The corresponding reaction is,



Thus, the eight pathways are identified for the secondary reactions of OH with 2,3-dimethylphenol. Of all the pathways studied, the pathway 5 leading to the formation of 3-hydroxy-2-methyl-2H-pyran-2-carbaldehyde is found to be the most favorable due to its small barrier of 7.74 kcal/mol.

B. Kinetics:

The results discussed in the previous section suggests that different secondary reactions could determine the overall reaction of 2, 3-dimethylphenol with OH. Hence, the rate of reaction corresponding to the formation of major byproducts from the oxidation reaction is crucial to determine the impact of dimethylphenol in the atmosphere. The rate constants are calculated using canonical variational transition state theory (CVT) with small curvature tunneling (SCT) corrections over the temperature range of 278-350 K with ZPE corrected energies, gradients and Hessians calculated at B3LYP/6-31G(d,p) level of theory. Since, no crossover has been observed between different reaction pathways, the overall rate constant can be calculated as the sum of the rate constants of each subsequent reaction. The results obtained for the formation of 3-hydroxy-2-methyl-2H-pyran-2-carbaldehyde (P5), which is the most favorable reaction are discussed below.

The formation of 3-hydroxy-2-methyl-2H-pyran-2-carbaldehyde consists of four reaction channels as described in Scheme 1. The rate constants for the formation of alkyl radical, peroxy radical, 3-methylphenol and the product channel are designated as k_a , k_b , k_c , and k_d , respectively. The overall rate constant k is the sum of the individual rate constants k_a , k_b , k_c , and k_d . These rate constants are summarized in Table 2 for the temperature range of 278-350 K. As given in Table 2, the rate constants k_a for the initial H-atom abstraction channel shows positive dependence on temperature. The calculated rate constant k_a for H-abstraction reaction at 298 K is $1.73 \times 10^{-13} \text{ cm}^3 \text{ molecule}^{-1} \text{ s}^{-1}$ which is quite comparable with the experimentally observed value of $8.3 \times 10^{-11} \text{ cm}^3 \text{ molecule}^{-1} \text{ s}^{-1}$. Earlier studies show that dimethylphenols are more reactive than dimethylbenzenes and trimethylbenzenes¹⁰. This is because both the methyl and hydroxyl groups donate electron density to the aromatic ring and activates the ring. The variation of k_a with temperature is very small which suggests that the activation energies around 298 K is close to zero.

The calculated rate constant k_b for the formation of peroxy radical is $8.81 \times 10^{-14} \text{ cm}^3 \text{ molecule}^{-1} \text{ s}^{-1}$ at 298 K. The calculated rate constants show a negative temperature dependence and this is due to the weak chemical bonding between the $\text{C}_6\text{H}_5\text{OHCH}_3(\text{CH}_2)$ and OO fragments in peroxy radical. Hence the reaction is reversible under tropospheric conditions and leads to chemical equilibrium between I1 and O_2 . The rate constant k_c calculated at 298 K for the formation of 3-methylphenol, along with formic acid and O_2 is $.2 \times 10^{-11} \text{ cm}^3 \text{ molecule}^{-1} \text{ s}^{-1}$. This rate constant value is comparable with the estimated rate constants for $\text{RO}_2 + \text{HO}_2$ reactions³⁷. The rate constant k_c increases with increase in temperature. The calculated rate constant k_d for the product channel is $5.51 \times 10^{-19} \text{ cm}^3 \text{ molecule}^{-1} \text{ s}^{-1}$ at 298 K. From the tabulated values, it has been observed that the rate constants k_d show a negative dependence on temperature. The overall rate constant k for the total reaction pathway is calculated as $2.22 \times 10^{-11} \text{ cm}^3 \text{ molecule}^{-1} \text{ s}^{-1}$ at 298 K. This value is in agreement with the experimental results obtained for the reactions of peroxy radicals with HO_2 ¹⁴. Thus the formation of intermediate channel I3 alone determines the overall reaction rate. This can be rationalized in terms of the structure of the peroxy radical. The $-\text{COO}-$ group in peroxy radical has high electron withdrawing character. Therefore, when it undergoes subsequent reactions, it becomes highly reactive towards the other atmospheric species. Thus, the peroxy radical serves as the key intermediate in OH initiated reactions of alkylated aromatic compounds. The Arrhenius expression fitting for the total rate constants over the temperature range of 278-350 K is $k = 3.55 \times 10^{-11} e^{-139/T} \text{ cm}^3 \text{ molecule}^{-1} \text{ s}^{-1}$ and the Arrhenius activation energy for the overall reaction is 16.82 kcal/mol. The Arrhenius plot of the total rate constant is shown in Figure 3. The tunneling effect is found to be significant only for the product channel with a tunneling energy of 86.33 kcal/mol. In general, the tunneling effect is important for H-atom abstraction reactions. But in this case, the energy barrier of the initial H-atom abstraction reaction is broad as suggested by a small imaginary vibrational frequency (-96.73 cm^{-1}) of the transition state TS1 and hence the tunneling effect is negligible. Since the overall rate constant decreases for increase in temperature, the reaction of 2,3-dimethylphenol with OH radical is significant in the lower layers of troposphere.

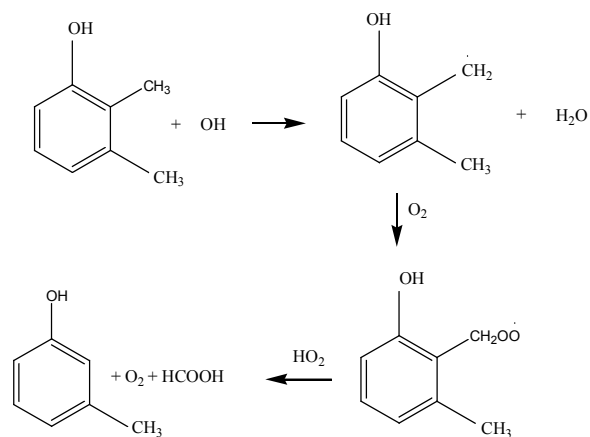
3. Conclusions

The potential energy surface, thermochemical and kinetic data for the reaction of 2, 3-dimethylphenol with OH reveal several important aspects of alkylated aromatic compounds in the atmospheric chemistry. From the present study, the following main conclusions are arrived.

1. The reaction between 2,3-dimethylphenol and OH radical is initiated by H-atom abstraction from methyl group and further reacts with O₂ to form a peroxy radical, a key intermediate in the reaction mechanism. This peroxy radical has excess energy to further undergo reaction with HO₂ in the atmosphere.
2. The reaction between peroxy radical of dimethylphenol and HO₂ proceeds by the loss of peroxy group, leading to the formation of 3-methylphenol, formic acid and O₂. The 3-methylphenol further undergoes oxidative degradation reaction with O₂. The reaction pathway corresponding to the formation of 3-hydroxy-2-methyl-2H-pyran-2-carbaldehyde is found to be the most favorable due to the small barrier of 7.74 kcal/mol and the rate constant is found to be $2.22 \times 10^{-11} \text{ cm}^3 \text{ molecule}^{-1} \text{ s}^{-1}$ at 298 K.
3. All the studied reaction channels are found to be exothermic at 298.15 K. The highest exothermicity of 85.12 kcal/mol is observed for the formation of 2-hydroxy-cyclohept-4-ene-1, 3-dione which supports autoignition and combustion processes.
4. The overall rate constant for all reactions show a negative temperature dependence, and hence the lifetime of dimethylphenol is expected to increase in the upper troposphere and lower stratosphere.
5. The results presented in this study allows for the elucidation of complete reaction mechanism and kinetics of the major products of alkylated aromatic compounds in the troposphere, thereby revealing the fact that the atmospheric radicals themselves attempt to degrade the pollutants in favor of life on earth.

4. Acknowledgement

One of the authors (K.S.) is thankful to the Department of Science and Technology (DST), India for granting the research project under DST-Fast track scheme for young scientists. L.S. is thankful to Bharathiar University for providing University Research Fellowship and Department of Science and Technology (DST), India for awarding INSPIRE Fellowship.



Scheme 1: Proposed reaction scheme for the reaction of 2,3-dimethylphenol with OH radical

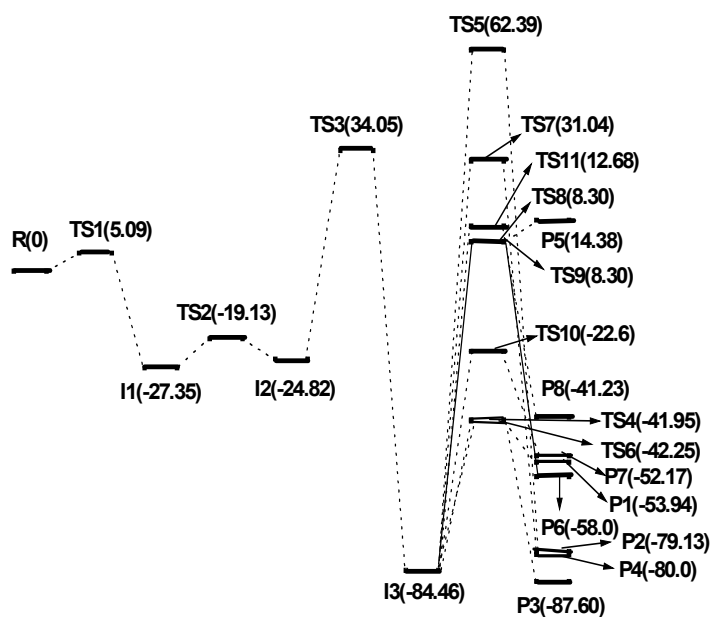
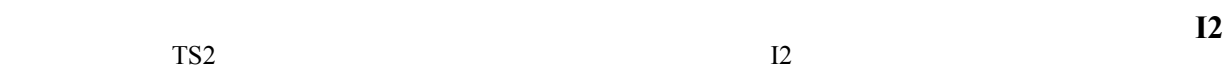
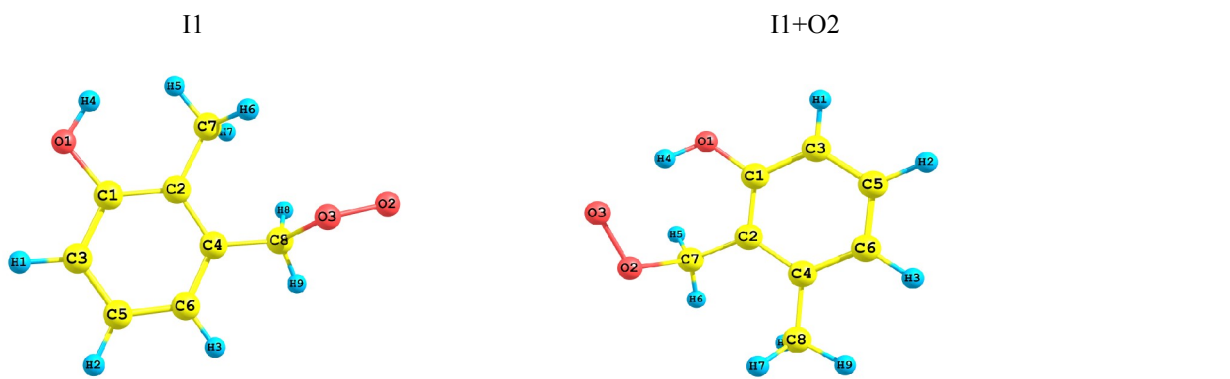
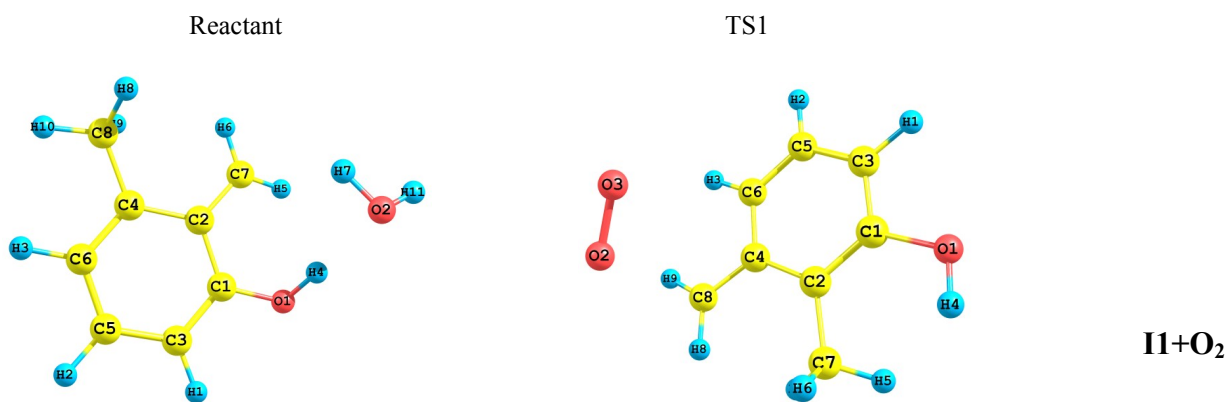
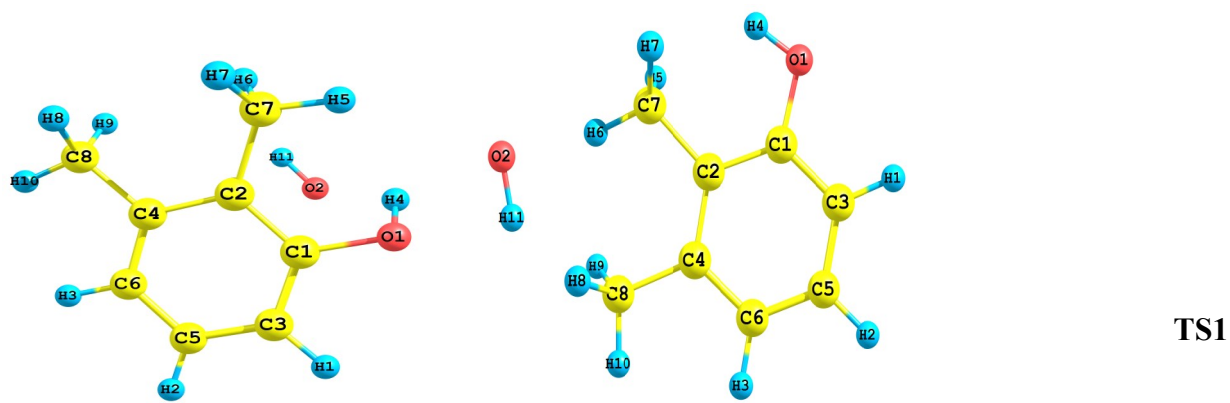


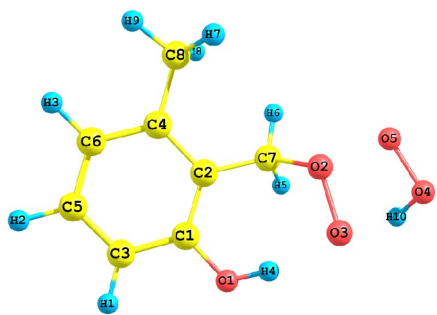
Figure 1: Potential energy surface for the proposed reactions of 2,3-dimethylphenol with OH radical. Relative energy (in kcal/mol) calculated at B3LYP/6-31 G(d,p) level of theory is given



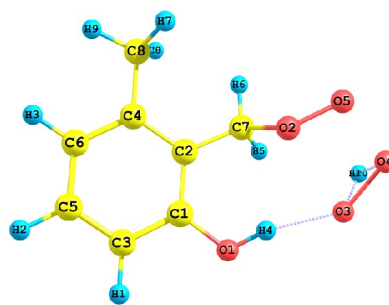
TS1

I1+O₂

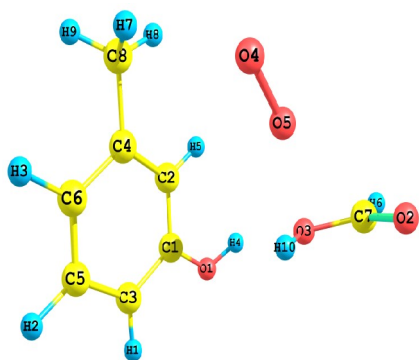
I2



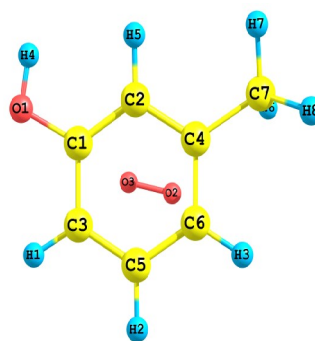
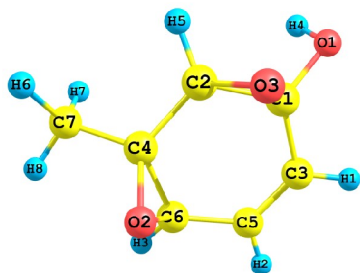
I2+HO2



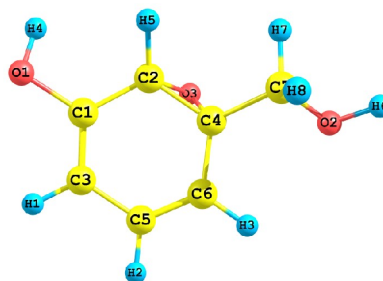
TS3



I3

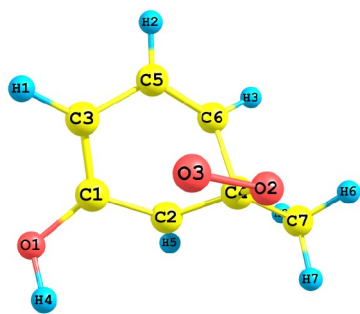
I3+O₂

TS4

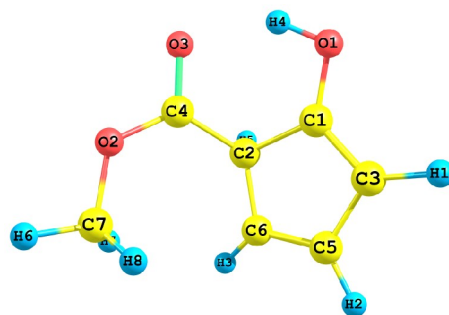


P1

P1

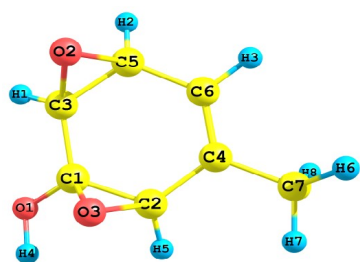


TS5

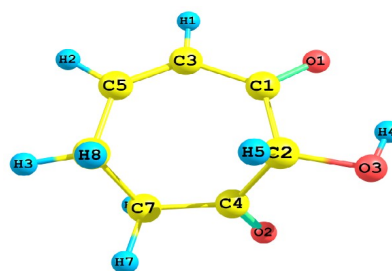


P2

P2

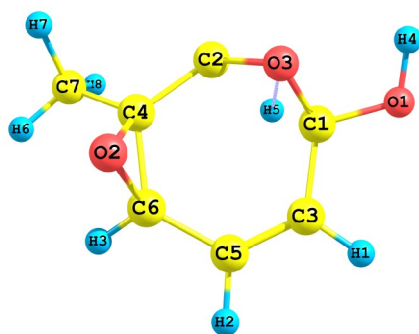


TS6

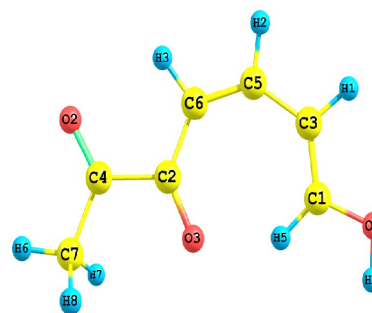


P3

P3

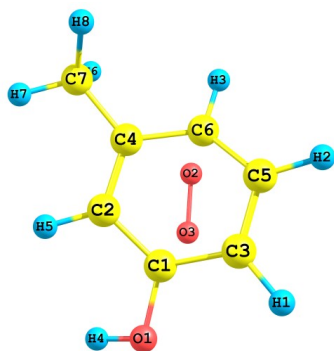


TS6

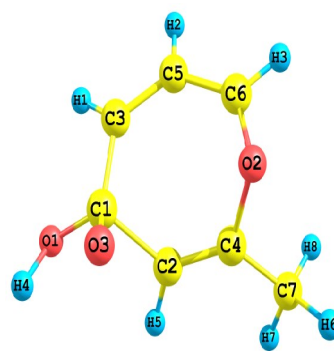


P3

P4

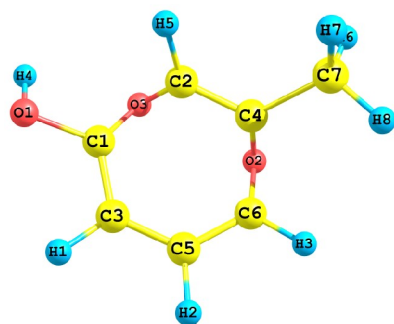


TS7

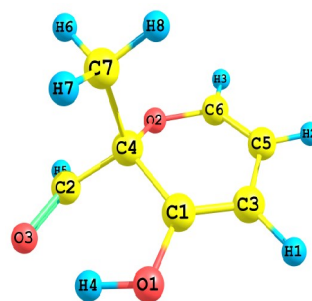


P4

TS8

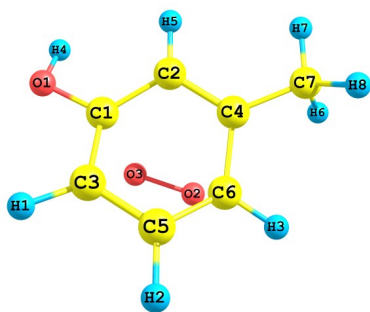


TS8

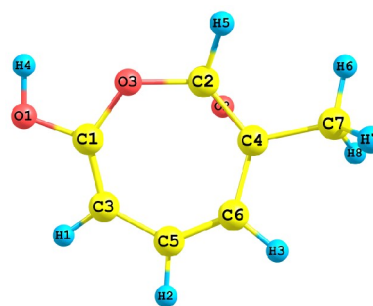


P5

P5

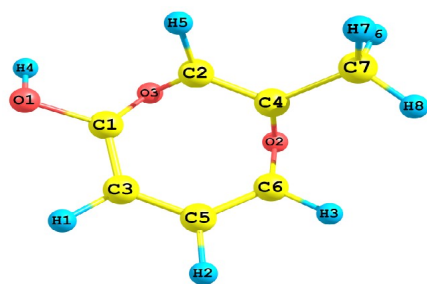


TS9

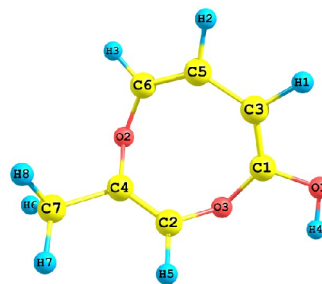


P6

P6

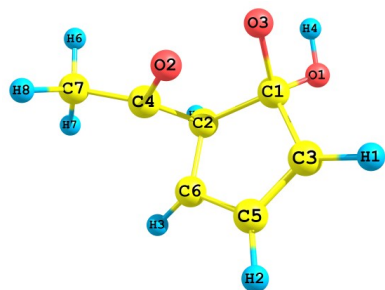


TS10

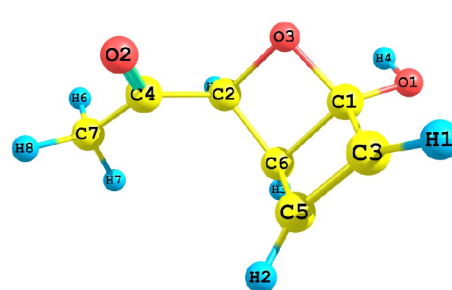


P7

P7



TS11



P8

P8

Figure 2: The optimized structure of the reactive species in the pathways corresponding to the reaction of 2,3-dimethylphenol with OH radical

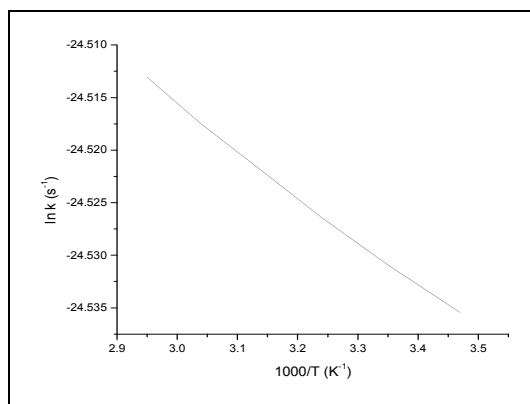


Figure 3: Arrhenius plot of the rate constants for the favorable reaction of 2,3-dimethylphenol with OH radical

Table 1: Relative energy (ΔE in kcal/mol) Enthalpy (ΔH in kcal/mol), Gibb's Free Energy (ΔG in kcal/mol) and Barrier height (in kcal/mol) for the proposed reactions of 2,3-dimethylphenol with OH radical

Pathways	Species	ΔE	Reactions	ΔH	ΔG	Barrier height
Initial step	R	0		-		
	TS1	5.09	$C_6H_5OH(CH_3)_2 + OH \rightarrow C_6H_5OHCH_3(C_2H_5) + H_2O$	27.35	0.9	3.94
	I1	-27.35			6.9	
	TS2	-19.13	$C_6H_5OHCH_3(CH_2) + O_2 \rightarrow C_6H_5OHCH_3(CH_2OO)$	-	-	-16.3
	I2	-24.82		-	4.31	30.51
	TS3	34.05	$C_6H_5OHCH_3(CH_2OO) + HO_2 \rightarrow C_6H_4OHCH_3 + O_2 + HCOOH$	86.02		
1	TS4	-41.95	$C_6H_4OHCH_3 + O_2 \rightarrow C_6H_4OHO(CH_2OH)$	-	3.56	-40.64
	P1	-53.94		51.87		
2	TS5	62.39	$C_6H_4OHCH_3 + O_2 \rightarrow C_5H_4OHCH_3O(C=O)$	-	3.18	60.80
	P2	-79.13		76.83		
3	TS6	-42.25	$C_6H_4OHCH_3 + O_2 \rightarrow C_5H_7OH(C=O)_2$	-	3.82	-40.57
	P3	-87.60		85.12		
4	TS7	31.04	$C_6H_4OHCH_3 + O_2 \rightarrow C_4H_4OHCH_3COH(C=O)$	-	0.19	29.40
	P4	-80.00		79.21		
5	TS8	8.30	$C_6H_4OHCH_3 + O_2 \rightarrow C_5H_3OHCH_3(CHO)$	-	2.88	7.74
	P5	14.38		71.94		
6	TS9	8.30	$C_6H_4OHCH_3 + O_2 \rightarrow C_4H_5OHCH_3(COC)_2$	-	3.09	8.39
	P6	-58.0		56.08		
7	TS10	-22.6	$C_6H_4OHCH_3 + O_2 \rightarrow C_4H_5OHCH_3(COC)_2$	-	2.22	-22.41
	P7	-52.17		50.61		
8	TS11	12.68	$C_6H_4OHCH_3 + O_2 \rightarrow C_5H_4OHO(OCCH_3)$	-	1.66	12.06
	P8	-41.23		40.43		

Table 2: Rate constants k_a , k_b , k_c and k_d (in $\text{cm}^3 \text{ molecule}^{-1} \text{ s}^{-1}$) for the individual reaction channels and overall rate constant k (in $\text{cm}^3 \text{ molecule}^{-1} \text{ s}^{-1}$) for the favorable reaction (Pathway 5) of 2,3-dimethylphenol with OH radical.

Temperature	$k_a \times 10^{-13}$	$k_b \times 10^{-14}$	$k_c \times 10^{-11}$	$k_d \times 10^{-19}$	$k \times 10^{-11}$
278	1.72	4.63	2.19	2.09	2.21
288	1.72	6.46	2.19	3.45	2.21
298	1.73	8.81	2.20	5.51	2.22
308	1.73	0.11	2.21	8.53	2.23
318	1.73	0.15	2.21	0.12	2.24
328	1.74	0.20	2.22	0.18	2.25
338	1.74	0.25	2.22	0.27	2.26
348	1.74	0.32	2.23	0.38	2.27
350	1.74	0.33	2.23	0.40	2.28

References

1. W. A. Lonneman, R. L. Seila and S. A. Meeks, Nonmethane organic composition in the Lincoln Tunnel., *Environ.Sci.Technol*, **20** (1986) 790.
2. S. Houweling, F. Dentener and J. Lelieveld, The impact of nonmethane hydrocarbon compounds on tropospheric photochemistry., *J. Geophys. Res.*, **103** (1998) 10673.
3. R. B. Zweideinger, J. E. Sigsby, S. B. Tejada, F. D. Stump, D. L. Dropkin, W. D. Ray and J. W. Duncan, Detailed hydrocarbon and aldehyde mobile source emissions from roadway studies., *Environ.Sci.Technol*, **22**(1988) 956.
4. R. Atkinson, Kinetics and Mechanisms of the Gas-Phase Reactions of the hydroxyl radical with Organic compounds., *J. Phys. Chem-Ref. Data, Monograph*, **1**(1994) 1.
5. R. Atkinson, Kinetics and Mechanisms of the Gas-Phase reactions of the hydroxyl radical with Organic compounds. *J. Phys. Chem-Ref. Data, Monograp*, **11**(989) 1.
6. R. G. Derwent, M. E. Jenkin and S. M. Saunders, Photochemical ozone creation potentials for a large number of reactive hydrocarbons under European conditions. *Atmos.Environ.*, **30** (1996)181.
7. J. H. Seinfeld and S. N. Pandis, Atmospheric Chemistry and Physics:From Air Pollution to Climate Change., *John Wiley&Sons, New York*, 1997.
8. J. G. Calvert, R. Atkinson, K. H. Becker, R. M. Kamens, J. H. Seinfeld, T. J. Wallington and G. Yarwood, Eds, The mechanisms of atmospheric oxidation of aromatic by hydrocarbons., *Oxford University Press, Oxford*, 2002.
9. R. Atkinson, K. R. Darnall, J. N. Pitts, Jr, Rate constants for the reactions of hydroxyl radicals and ozone with cresols at 300K., *J. Phys. Chem.*, **82** (1978) 2759.

10. L. P. Thuner, P. Bardini, G. J. Rea and J. C. Wenger, Kinetics of the gas phase reactions of OH and NO₃ radicals with dimethylphenols., 2004.
11. C. C. Tourneur, F. Henry, M. A. Janquin, L. Brutier, Gas-phase reaction of hydroxyl radicals with m-, o- and p-cresol., *Int. J. Chem. Kinet*, **38**(2006) 9.
12. T. H. Lay, J. W. Bozzelli and J. H. Seinfeld, Atmospheric Photochemical Oxidation of Benzene: Benzene+OH and the Benzene-OH adduct (Hydroxyl-2,4-cyclohexadienyl) + O₂., *J. Phys. Chem.*, **100** (1996) 6543.
13. R. Atkinson, S. M. Aschmann, *Int. J. Chem. Kinet*, **26** (1994) 929.
14. B. Bohn, C. Zetzsch, Gas-phase reaction of the OH-benzene adduct with O₂, reversibility and secondary formation of HO₂. *Phys. Chem. Chem. Phys.*, **1**(1999) 5097.
15. P. Khare, N. Kumar, K. M. Kumari and S. S. Srivastava, Atmospheric formic and acetic acids: An overview., *Rev. Geophys.*, **37** (1999) 227.
16. R. Volkamer, U. Platt and K. Wirtz, *J. Phys. Chem. A.*, **105** (2001)7865.
17. E. C. Tuazon, H. Macleod, R. Atkinson, W. P. L. Carter, a-Dicarbonyl yields from the NO_x-air photooxidation of a series of aromatic hydrocarbons in air., *Environ.Sci.Technol*, **20** (1986) 383.
18. C. Lee, W. Yang and R. G. Parr, *Phys.Rev B* **37** (1988) 785.
19. A. D. Becke, Density-functional thermochemistry III-The role of exact exchange., *J. Chem. Phys.*, **98** (1993) 5648.
20. J. M. Anglada, Complex mechanism of the gas phase reaction between formic acid and hydroxyl radical. Proton coupled electron transfer versus radical hydrogen abstraction mechanisms. *J. Am. Chem. Soc.*, **126** (2004) 9809.
21. D. Zhang and R. Zhang, Mechanism of OH formation from the ozonolysis of isoprene: A quantum chemical study., *J. Am. Chem. Soc.*, **124** (2002) 2692.
22. C. Gonzalez, H. B. Schlegel, An improved algorithm for reaction path following., *J. Chem. Phys.*, **90** (1989) 2154.
23. C. Gonzalez and H. B. Schlegel, Reaction path following in mass-weighted internal coordinates., *J. Chem. Phys.*, **94** (1990) 5523.
24. M. J. Frisch, G. W. T., H. B. Schlegel, G. E. Scuseria, M. A. Robb, J. R. Cheeseman, G. Scalmani, V. Barone, B. Mennucci, G. A. Petersson, H. Nakatsuji, M. Caricato, X. Li, H. P. Hratchian, A. F. Izmaylov, J. Bloino, G. Zheng, J. L. Sonnenberg, M. Hada, M. Ehara, K. Toyota, R. Fukuda, J. Hasegawa, M. Ishida, T. Nakajima, Y. Honda, O. Kitao, H. Nakai, T. Vreven, J. A. Montgomery, Jr., J. E. Peralta, F. Ogliaro, M. Bearpark, J. J. Heyd, E. Brothers, K. N. Kudin, V. N. Staroverov, R. Kobayashi, J. Normand, K. Raghavachari, A. Rendell, J. C. Burant, S. S. Iyengar, J. Tomasi, M. Cossi, N. Rega, J. M. Millam, M. Klene, J. E. Knox, J. B. Cross, V. Bakken, C. Adamo, J. Jaramillo, R. Gomperts, R. E. Stratmann, O. Yazyev, A. J. Austin, R. Cammi, C. Pomelli, J. W. Ochterski, R. L. Martin, K. Morokuma, V. G. Zakrzewski, G. A. Voth, P. Salvador, J. J. Dannenberg, S. Dapprich, A. D. Daniels, O. Farkas, J. B. Foresman, J. V. Ortiz, J. Cioslowski, and D. J. Fox, , *Gaussian 09, Revision A.02.*, Gaussian, Inc., Wallingford CT, 2009.
25. B. C. Garrett, D. G. Truhlar, R. S. Grev and A. W. Magnuson, Improved treatment of threshold contributions in variational transition state theory., *J. Phys. Chem.*, **84** (1980) 1730.
26. B. C. Garrett and D. G. Truhlar, Generalized transition state theory, Bond energy-bond order method for canonical variational calculations with application to hydrogen atom transfer reactions., *J. Am. Chem. Soc.*, **101** (1979) 4534.

27. Y. P. Liu, G. C. Lynch, T. N. Truong, D. H. Lu, D. G. Truhlar and B. C. Garrett, Molecular modeling of the kinetic isotope effect for the [1,5]-sigmatropic rearrangement of cis-1,3-pentadiene. *J. Am. Chem. Soc.*, **115** (1993) 2408.
28. D. H. Lu, T. N. Truong, V. S. Melissas, G. C. Lynch, Y. P. Liu, B. C. Garrett, R. Steckler, A. D. Issacson, S. N. Rai, G. C. Hancock, J. G. Louderdale; T. Joseph and D. G. Truhlar, Polyrate 4: A new version of a computer program for the calculation of chemical reaction rates for polyatomics *Comput. Phys. Commun.*, **71** (1992) 235.
29. Y. Y. Chuang and D. G. Truhlar, Stastical thermodynamics of bond torsional modes. *J. Chem. Phys.*, **11** (2000) 1221.
30. J. Zheng, S. Zhang, J. C. Corchado, Y. Y. Chuang, E. L. Coitino, B. A. Ellingson and D. G. Truhlar, *GAUSSRATE version 2009*.
31. J. Zheng, S. Zhang, B. J. Lynch, J. C. Corchado, Y. Y. Chaung, P. L. Fast, W. P. Hu, Y. P. Liu, G. C. Lynch, K. A. Nguyen, C. F. Jackels, A. F. Ramos, B. A. Ellingson, V. S. Melissas, J. Villa, I. Rossi, Coitino, E. L. Pu and T. V. Albu, *POLYRATE version 2010*.
32. E. S. C. Kwok, S. M. Aschmann, R. Atkinson and J. Arey, Products of the gas-phase reactions of o-, m-, and p-xylene with the OH radical in the presence and absence of NO_x. *Faraday Transactions* 1997, 7.
33. I. Barnes, J. Hjorth and N. Mihalopoulos, *Chem. Rev.*, **106** (2006) 940.
34. Z. Li, P. Nguyen, M. F. Leon, J. H. Wang, K. Han and G. Z. He, *J. Phys. Chem. A*, **110** (2006) 2698.
35. M. B. Williams, P. C. Jost, B. M. Cossairt and A. J. Hynes, *J. Phys. Chem. A*, **111** (2007) 89.
36. G. D. Silva, M. R. Hamdan and J. W. Bozzelli, Oxidation of the benzyl radical: Mechanism, Thermochemistry and Kinetics for the reactions of benzyl hydroperoxide., *J. Chem. Theory Comput.*, **5** (2009) 3185.
37. N. I. Butkovskaya and L. G. Bras, *J. Phys. Chem.*, **98**, (1994) 2582.